How to cite: Angew. Chem. Int. Ed. 2023, e202309259
doi.org/10.1002/anie.202309259

Polymer Folding Hot Paper

Visible-Light-Induced Control over Reversible Single-Chain Nanoparticle Folding

Patrick H. Maag, Florian Feist, Vinh X. Truong, Hendrik Frisch, Peter W. Roesky,* and Christopher Barner-Kowollik**

Abstract: We introduce a class of single-chain nanoparticles (SCNPs) that respond to visible light (λ_{max} = 415 nm) with complete unfolding from their compact structure into linear chain analogues. The initial folding is achieved by a simple esterification reaction of the polymer backbone constituted of acrylic acid and polyethylene glycol carrying monomer units, introducing bimane moieties, which allow for the photochemical unfolding, reversing the ester-bond formation. The compaction and the light driven unfolding proceed cleanly and are readily followed by size exclusion chromatography (SEC) and diffusion ordered NMR spectroscopy (DOSY), monitoring the change in the hydrodynamic radius (R_H). Importantly, the folding reaction and the light-induced unfolding are reversible, supported by the high conversion of the photo cleavage. As the unfolding reaction occurs in aqueous systems, the system holds promise for controlling the unfolding of SCNPs in biological environments.

Introduction

In the last decade, single-chain nanoparticles (SCNPs) have evolved into a fascinating research field.[1] Research teams from all over the world contribute[2] and design soft-shell particles with precise control over structure and functionality extending the range of SCNPs for application in many fields including catalysis,[3] sensing[4] or biomedical applications.[5]

An emerging field for SCNPs are biomedical applications, enabled by their similar size (3–20 nm) and structure compared to proteins. The field benefits from the large variety of functional SCNPs prepared from water-soluble and biocompatible polymer precursors, which are typically designed for uses in drug delivery, target imaging and enzyme mimicry.[6] Previous studies show that the size of the SCNPs is an important parameter in biomedical applications as it influences their cellular uptake[7] and renal clearance[8] in biological systems. Remote control over particle size and shape would thus provide control over cell interactions and biodistribution behavior with temporal and spatial resolution, improving the potential of controlled drug delivery as well as selective cell labeling and imaging.[9] Current approaches for remotely controlled SCNP folding and unfolding are very rare and are not applicable for biomedical applications as they are incompatible with water[10] or require the addition of organic solvents as a trigger.[11] Due to its high spatiotemporal control, light is an ideal trigger to control the unfolding of SCNPs. For biological applications, visible light is required to minimize photodamage and enable maximum tissue penetration, which limits the number of photochemical reactions available.[12] In addition, the confined environment within the SCNP has a drastic effect on the photoreaction kinetics.[13] [2+2] photocycloadditions, for example, are - within the steric confines of SCNPs - kinetically more favored than the corresponding photocycloreversion, preventing photocycloreversion based unfolding of SCNPs.[14] Within biological applications, one is further restricted to visible light to avoid degradation of biomolecules which consequently limits the number of options.[12] A different approach to remotely control bio-

[*] P. H. Maag, Dr. H. Frisch, Prof. C. Barner-Kowollik
School of Chemistry and Physics, Queensland University of Technology (QUT), 2 George Street,
4000 Brisbane, QLD (Australia)
and
Centre for Materials Science, Queensland University of Technology (QUT), 2 George Street
4000 Brisbane, QLD (Australia)
E-mail: h.frisch@qut.edu.au
christopher.barnerkowollik@qut.edu.au

P. H. Maag, Prof. P. W. Roesky
Institute of Inorganic Chemistry, Karlsruhe Institute of Technology (KIT)
Engesserstraße 15, 76131 Karlsruhe (Germany)
E-mail: roesky@kit.edu

P. H. Maag, Dr. F. Feist, Prof. C. Barner-Kowollik
Institute of Nanotechnology (INT), Karlsruhe Institute of Technology (KIT)
Hermann-von-Helmholtz-Platz 1, 76344 Eggenstein-Leopoldshafen (Germany)

Dr. V. X. Truong
Institute of Sustainability for Chemicals, Energy and Environment (ISCE2), Agency for Science, Technology and Re-search (A*STAR)
1 Pesek Road, Jurong Island, Singapore 627833 (Republic of Singapore)

logical functions was presented by Herrmann and co-workers, who developed a method to reactivate thrombin using ultrasound to cleave the interactions between polyaptamer and the enzyme, restoring its catalytic activity.[15]

Herein, we introduce a key SCNP functionality, i.e. controlling the compaction of defined macromolecules remotely by visible light. Using bimane as photolabile linkage points enables the cleavage under mild conditions, resulting in an unfolded and reusable polymer (Scheme 1). Initially characterized by Kosower and co-workers as a class of heterocyclic molecules, bimanes are of specific interest as fluorescent photocleavable linkers.[16] We demonstrate their utility in the controlled folding and unfolding of a water soluble single polymer chain. Expanding the potential of SCNPs towards biocompatibility, we design a water-soluble system with fluorescent moieties that is suitable for tracing and imaging.[17]

Results and Discussion

Below we exemplify our strategy for unfolding of SCNPs by visible light affording the original linear polymer and allowing subsequent refolding, exploiting fluorescent bimane moieties as cross-linking units which are photocleavable under visible light (Scheme 1).

The polymeric backbone was synthesized by reversible addition fragmentation chain transfer (RAFT) copolymerization of poly(ethylene glycol) methyl ether methacrylate (MPEGMA, $M_n = 300\ g\,mol^{-1}$) and acrylic acid (AA) with a monomer composition of 16 % AA calculated from the conversion of the monomers during polymerization, monitored by ^1H NMR spectroscopy using DMF as reference (refer to the Supporting Information, section 2.6). Subsequently, the RAFT end-groups were hydrolyzed to form hydroxy groups (refer to the Supporting Information, section 2.4)[18] affording poly(MPEGMA-*co*-AA) (**P1**, $M_n = 36.53\ 10^3\ g\,mol^{-1}$, $D = 8.53 \pm 0.23\ 10^{-11}\ m^2\,s^{-1}$, $R_H = 4.62 \pm 0.13$ nm, $x_{AA} = 16$ %). The apparent molecular weight (M_n) was determined by size exclusion chromatography (SEC) based on the hydrodynamic volume of the polymer in dimethylacetamide. To support these data, the diffusion coefficient, D, was determined by diffusion-ordered spectroscopy (DOSY) in deuterated chloroform and therefrom the hydrodynamic radius (R_H) was calculated using the Stokes–Einstein equation.

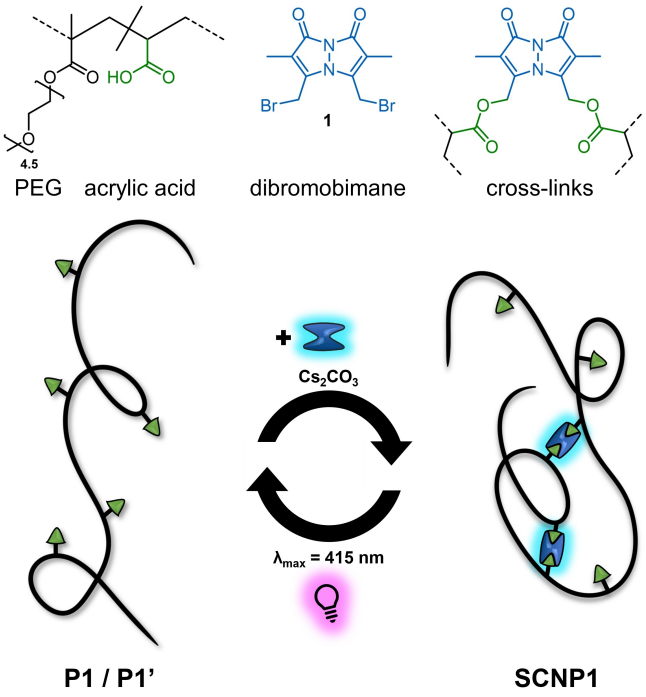

Scheme 1. Folding and unfolding of poly(MPEGMA-*co*-acrylic acid) utilizing dibromobimane **1** as fluorescent, photoreactive cross-linker. In the folding reaction, the acrylic acid (AA) units react in a base-mediated S_N2 reaction with **1**. The generated cross-links can be cleaved by visible light resulting in the original polymer and dihydroxybimane **2**.

The obtained polymer was folded into SCNPs by an esterification reaction of the carboxylic acid pendant groups with dibromobimane **1** in a highly diluted solution in tetrahydrofuran (THF, $0.2\ mg\,mL^{-1}$) and cesium carbonate as base (**SCNP1**, $M_n = 31.34\ 10^3\ g\,mol^{-1}$, $D = 1.14 \pm 0.05\ 10^{-10}\ m^2\,s^{-1}$, $R_H = 3.46 \pm 0.16$ nm). During folding, the hydrodynamic volume of the polymer decreases, resulting in a decrease of the apparent molecular weight by 17 % (refer to SEC, Figure 1), leading to a shift of the **SCNP1** SEC retention time compared to the **P1** (red arrow). The folding was further monitored by the UV/Vis absorption of the polymer in the SEC trace relative to the refractive index detection (RID). We find that the absorption at 400 nm increases linearly over time, evidencing the incorporation of bimane units within the polymer chain and correlates with the decrease in apparent molecular weight, demonstrating that the bimanes act as cross-links. The linear increase of absorption might occur from the low concentration of bimane and carboxylic acid pendant groups in THF, resulting in a concentration independent trend. A higher bimane ratio would lead to an increased reaction rate, but also incorporate single bound bimanes which do not contribute to cross-linking.

Subsequently, the fluorescent **SCNP1** was unfolded by irradiating with $\lambda_{max} = 415$ nm in water, cleaving the ester bonds and releasing dihydroxybimane **2** and the original polymer with carboxylic acid groups (**P1′**, $M_n = 37.29\ 10^3\ g\,mol^{-1}$, $D = 6.97 \pm 0.20\ 10^{-11}\ m^2\,s^{-1}$, $R_H = 5.65 \pm 0.17$ nm). During irradiation the unfolding of **SCNP1** is evidenced by an increase in the hydrodynamic volume, which concomitantly results in an increase in the apparent molecular weight by 19 % (SEC), which is visually observed by a shift of the **P1′** SEC trace compared to **SCNP1** (blue arrow). It appears that the shift for the unfolding (towards **P1′**) in the SEC trace is not as significant as the initial folding, even though the molecular weight is similar of both polymers (**P1**, **P1′**, refer to SEC, Figure 1). The incomplete unfolding is possibly caused by a small amount of remaining bimane cross-links along the chain or side reaction occurring during the photocleavage between bimane units. The small shift may also be caused by the alteration of the interaction with the SEC column by a change in functional group density.

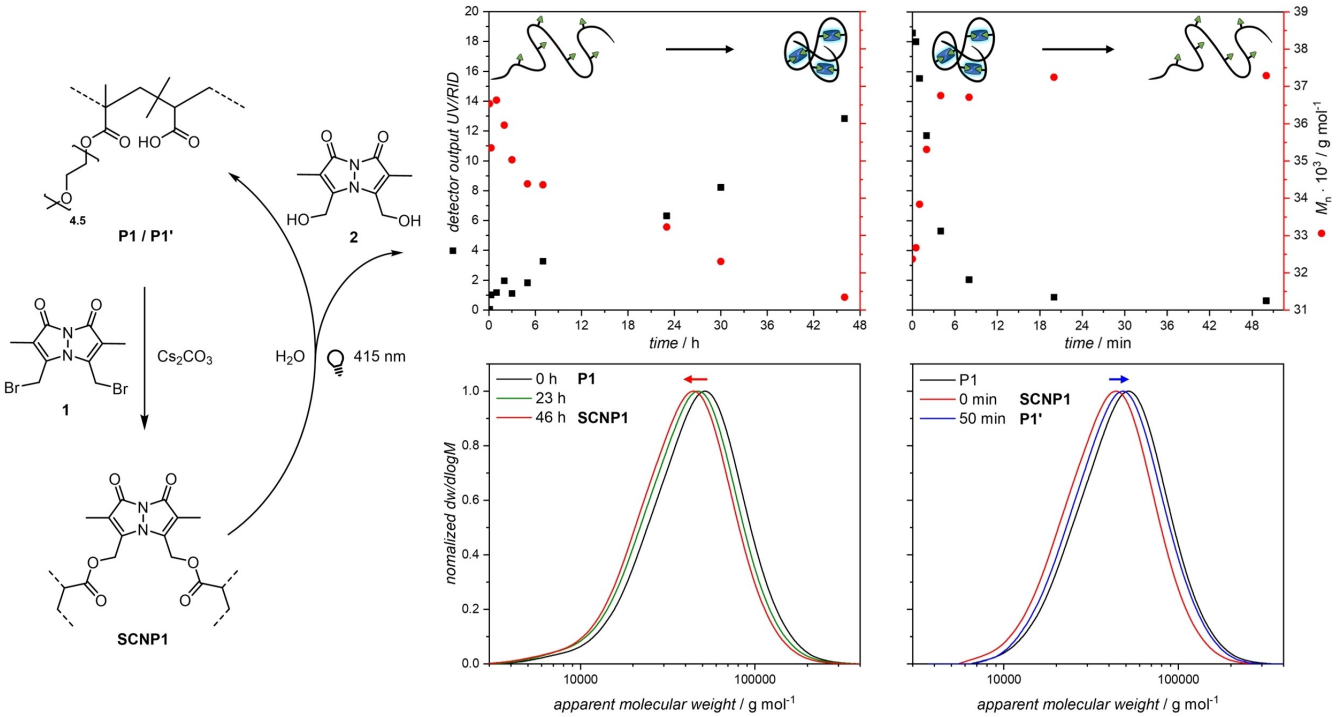

Figure 1. Left: Synthetic route for folding poly(MPEGMA-*co*-acrylic acid) (**P1**) with dibromobimane **1** in an esterification reaction with AA units and cesium carbonate as base resulting in **SCNP1**. The bimane caged esters - functioning as cross-links - can be cleaved by visible light, resulting in the original polymer and dihydroxybimane **2** as side product. Top middle: Kinetics of the folding of **P1** to **SCNP1** monitored by UV/Vis absorption at 400 nm and apparent molecular weight by size exclusion chromatography (SEC). The cross-linking of the polymer chain leads to a higher compaction and consequently to a smaller hydrodynamic volume appearing with a smaller apparent molecular weight in the SEC. Bottom middle: RID SEC traces of **P1** folding to **SCNP1**. Top right: Kinetics of the unfolding of **SCNP1** to **P1′** by irradiation with visible light monitored by UV/Vis absorption at 400 nm and apparent molecular weight by SEC. The cleavage of the cross-links leads to unfolding and consequently to a higher hydrodynamic volume appearing with a higher apparent molecular weight in the SEC. Bottom right: RID SEC traces of **SCNP1** unfolding to **P1′** compared to **P1**.

During the unfolding, the UV/Vis absorption of the polymer in the SEC trace decreases asymptotically to zero with irradiation time, indicating nearly full cleavage of the bimane units from the SCNP, correlating with an increase of the apparent molecular weight. In addition, the release of the carboxylic acid groups by photocleavage was also monitored by measuring pH during the unfolding. Similar to the kinetics monitored using absorption and molecular weight, the pH decreases rapidly, indicating the release of the carboxylic acid groups and a full recovery of the original polymer (refer to the Supporting Information, section 2.5).

Furthermore, we estimated the number of bimane units per polymer chain by comparing the molar absorption coefficient of the bimane caged acetate ester (**3**, $\varepsilon_{385nm} = 5.91 \pm 0.38\ 10^3\ L\,mol^{-1}\,cm^{-1}$) (as a close model of the bimane units in the SCNPs) with the absorption spectra of **SCNP1** and **P1′**. Based on the molecular weight of the polymers calculated from the conversion of the polymerization of close to $74\ kg\,mol^{-1}$, **SCNP1** was determined to feature 18.5 ± 0.6 bimane units per polymer chain. In comparison, **P1′** was estimated to have 3.6 ± 0.2 bimane units per chain, which is a decrease of 80 % after 20 min of irradiation (refer to the Supporting Information, section 2.10.1). A high degree of unfolding after a cleavage of 80 % bimane units is supported by a Monte Carlo simulation, modelling the probability of single or double bonded bimane units. Experimental results of the photocleavage of **3** over time show similar composition of single (**4**) and double (**2**) cleaved bimanes. According to both approaches, only one quarter of the remaining 20 % bimane units are double bonded (i.e., representing cross-links), whereas the other three quarters are cleaved on one side and do not cross-link the polymer chain anymore (refer to the Supporting Information, section 2.10.2–3). The folding and unfolding can be also monitored by ^{1}H NMR spectroscopy of the bimane resonances compared to the backbone, yet NMR spectroscopy cannot be used to calculate the exact cross-linking density due to an enhanced experimental uncertainty. The same applies to the resonances of the cleaved dihydroxybimane **2** after irradiating **SCNP1** for 20 min with a 415 nm LED in D_2O (refer to the Supporting Information, section 2.9).

The observed changes in the molecular weight were confirmed by DOSY measurements. The diffusion coefficient, D, increase by close to 34 % after crosslinking, and consequently the calculated R_H decreases from 4.62 ± 0.13 nm (**P1**) to 3.46 ± 0.16 nm (**SCNP1**, Figure 2). After irradiation, D decreases by 63.5 % resulting in an increased R_H of 5.65 ± 0.17 nm (**P1′**).

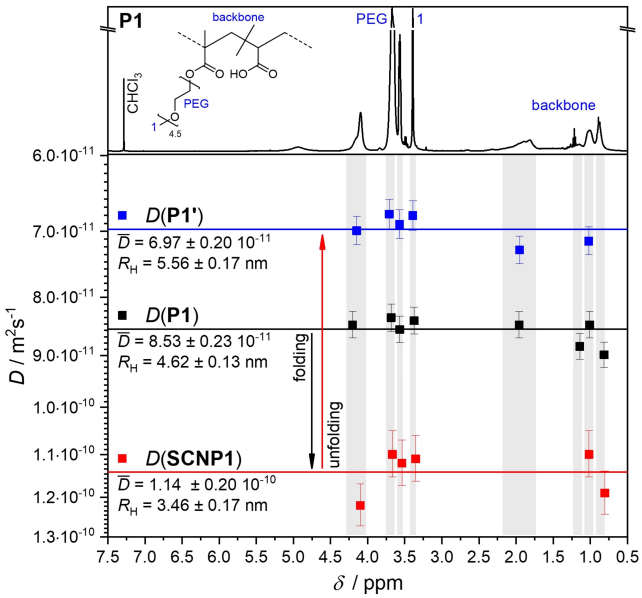

Figure 2. Diffusion coefficients (*D*) determined by diffusion-ordered spectroscopy (DOSY) in deuterated chloroform of integrated polymer resonances for the original polymer **P1**, the folded **SCNP1** and the unfolded **P1′**. The defined integrals are compared with the ^{1}H NMR spectrum of **P1** displayed above. The *D* of the corresponding chemical shifts is displayed as a colored square (■) within the integral areas. For each polymer, the arithmetic mean was calculated and displayed as a colored line (–), wherefrom the hydrodynamic radius (R_H) was calculated. *D* increased after folding, correlated with a smaller R_H and decreases after irradiation, indicating an unfolding of the SCNPs.

We hypothesize that the higher R_H is due to a similar reason as the smaller shift in the SEC trace. Small leftovers of bimane units lead to a different hydrodynamic volume in different solvents as dimethylacetamide for SEC compared to chloroform for DOSY (refer to Supporting Information, section 5). The fluorescence of the bimane cross-links also provides a visual indication of the folding and unfolding showing a strong emission at around 470 nm (λ_{ex} = 395 nm) also visible under a TLC-UV lamp (Figure 3). Compared to the SCNPs, the unfolded polymers only display a low intensity of around 5 % after purification by dialysis, which is caused by residual bimane moieties (primarily single bonded according to the Monte Carlo simulation). The purified **SCNP1** and unfolded **P1′** are showing a similar fluorescence spectrum as well as the fluorescence spectra of the bimane derivates obtained in small molecule synthesis and irradiation experiments (refer to Supporting Information, section 2.7 and 2.8). It was also shown that the dihydroxybimane **2** is stable under irradiation.

A key advantage of our herein introduced system is the reusability of the obtained polymer (**P1′**) after unfolding. We were able to repeat the cycle a second time, after obtaining the crude polymer by freeze drying, under the same conditions as employed for the first cycle described in the Supporting Information, section 2.3 and 2.4. **SCNP1′** is obtained after the second folding cycle and **P1″** after a second unfolding, which shows that the carboxylic acid groups were successfully released and allow for the reuse of the polymer. The shifts in the SEC retention times during the second cycle are similar to the shifts in the first cycle, resulting in alternating molecular weights after folding and unfolding. Concomitantly, the UV/Vis absorption increases with every folding and decreases with unfolding, indicating the release and installation of bimane cross-links.

Conclusion

Driven by the need to design single-chain nanoparticles (SCNPs) that are able to unfold with mild triggers, we have herein introduced SCNPs that can be fully unfolded using visible light. In addition, the reconstituted open polymer chains can be effectively refolded into SCNPs. Importantly, the unfolding functions in water under mild conditions enabling further use in biological applications. We submit that the current advance in our ability to fold and unfold SCNPs with a mild external trigger may allow to manipulate SCNPs in their geometry inside biological systems.

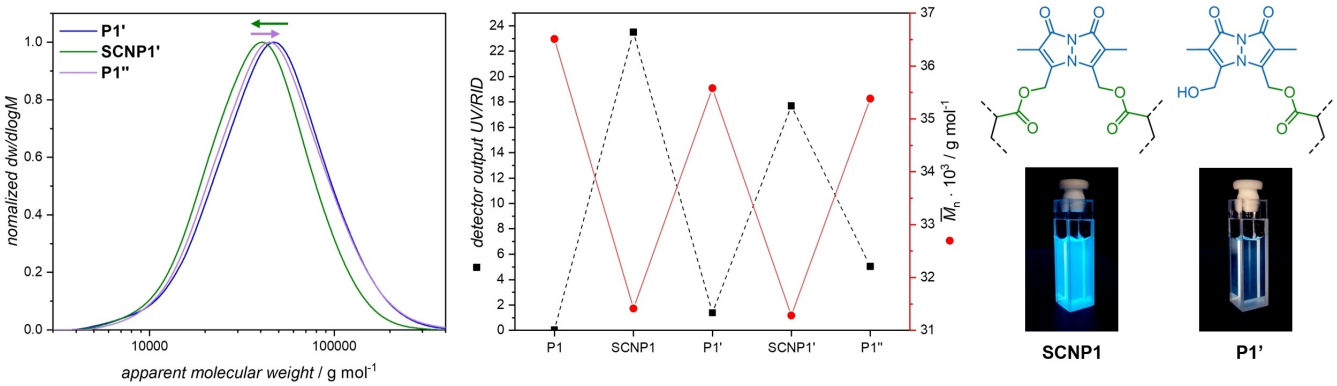

Figure 3. Folding of poly(MPEGMA-*co*-acrylic acid) (**P1**) with dibromobimane **1** and unfolding with visible light in a repetitive fashion. Left: The second cycle shows a similar shift of the SEC trace compared to the first cycle (Figure 1) resulting in a lower apparent molecular weight for **SCNP1′** and increasing apparent molecular weight for **P1″**. Middle: Depictures the apparent molecular weight and absorption at 400 nm for every step in the cycle showing alternating values. Right: Fluorescence of **SCNP1** and **P1** in water under a UV lamp showing a lower intensity after unfolding.

Acknowledgements

C.B.-K. acknowledges funding by the Australian Research Council (ARC) in the form of a Laureate Fellowship enabling his photochemical research program. H.F. is grateful for a DECRA Fellowship from the ARC. C.B.-K. and H.F. acknowledge continuous support by QUT's Centre for Materials Science. All authors acknowledge QUT's Central Analytical Research Facility (CARF) supported by QUT's Research Portfolio. P.H.M. acknowledges financial support from the Karlsruhe Institute of Technology (KIT). The authors acknowledge Dr. Aaron Micallef (QUT) for recording and optimizing the DOSY NMR measurements, Dr. David Marshall (QUT) for his support with LC-MS measurements, Dr. Daniel Kodura (QUT) for his pre-experiments that preceded the project, as well as Rita Michenfelder (QUT/KIT) for her support with HPLC fluorescence measurements, Sebastian Gillhuber (QUT/KIT) for his support with statistics and coding, and Fred Pashley-Johnson (QUT/Ghent University) for his support with analytical and synthetic questions. Open Access publishing facilitated by Queensland University of Technology, as part of the Wiley - Queensland University of Technology agreement via the Council of Australian University Librarians.

Conflict of Interest

The authors declare no conflict of interest.

Data Availability Statement

The data that support the findings of this study are available in the supplementary material of this article.

Keywords: Bimanes · Reversible Polymer Folding · Single-Chain Nanoparticles · Visible Light Photochemistry

[1] a) K. Mundsinger, B. T. Tuten, L. Wang, K. Neubauer, C. Kropf, M. L. O'Mara, C. Barner-Kowollik, *Angew. Chem. Int. Ed.* **2023**, *62*, e202302995; b) J. Chen, J. Wang, Y. Bai, K. Li, E. S. Garcia, A. L. Ferguson, S. C. Zimmerman, *J. Am. Chem. Soc.* **2018**, *140*, 13695–13702; c) Y. Shao, Y. L. Wang, Z. Tang, Z. Wen, C. Chang, C. Wang, D. Sun, Y. Ye, D. Qiu, Y. Ke, *Angew. Chem. Int. Ed.* **2022**, *61*, e202205183.

[2] a) A. M. Hanlon, C. K. Lyon, E. B. Berda, *Macromolecules* **2016**, *49*, 2–14; b) J. A. Pomposo, *Single-Chain Polymer Nanoparticles: Synthesis*, *Characterization*, *Simulations*, *and Applications*, Wiley, Hoboken, **2017**.

[3] J. Chen, K. Li, J. S. L. Shon, S. C. Zimmerman, *J. Am. Chem. Soc.* **2020**, *142*, 4565–4569.

[4] D. Kim, P. V. Pikhitsa, H. Yang, M. Choi, *Nanotechnology* **2011**, *22*, 485501.

[5] X. Tian, R. Xue, F. Yang, L. Yin, S. Luan, H. Tang, *Biomacromolecules* **2021**, *22*, 4306–4315.

[6] A. P. P. Kröger, J. M. Paulusse, *J. Controlled Release* **2018**, *286*, 326–347.

[7] X. Chen, R. Li, S. H. D. Wong, K. Wei, M. Cui, H. Chen, Y. Jiang, B. Yang, P. Zhao, J. Xu, *Nat. Commun.* **2019**, *10*, 2705.

[8] M. Longmire, P. L. Choyke, H. Kobayashi, *Nanomedicine* **2008**, *3*, 703–717.

[9] a) C.-C. Cheng, S.-Y. Huang, W.-L. Fan, A.-W. Lee, C.-W. Chiu, D.-J. Lee, J.-Y. Lai, *ACS Appl. Polym. Mater.* **2021**, *3*, 474–484; b) A. P. P. Kröger, N. M. Hamelmann, A. Juan, S. Lindhoud, J. M. Paulusse, *ACS Appl. Mater. Interfaces* **2018**, *10*, 30946–30951.

[10] a) D. Kodura, H. A. Houck, F. R. Bloesser, A. S. Goldmann, F. E. Du Prez, H. Frisch, C. Barner-Kowollik, *Chem. Sci.* **2021**, *12*, 1302–1310; b) A. Levy, R. Feinstein, C. E. Diesendruck, *J. Am. Chem. Soc.* **2019**, *141*, 7256–7260.

[11] P. J. Stals, C.-Y. Cheng, L. van Beek, A. C. Wauters, A. R. Palmans, S. Han, E. Meijer, *Chem. Sci.* **2016**, *7*, 2011–2015.

[12] K. A. Ryu, C. M. Kaszuba, N. B. Bissonnette, R. C. Oslund, O. O. Fadeyi, *Nat. Chem. Rev.* **2021**, *5*, 322–337.

[13] a) D. Kodura, L. L. Rodrigues, S. L. Walden, A. S. Goldmann, H. Frisch, C. Barner-Kowollik, *J. Am. Chem. Soc.* **2022**, *144*, 6343–6348; b) H. Frisch, J. P. Menzel, F. R. Bloesser, D. E. Marschner, K. Mundsinger, C. Barner-Kowollik, *J. Am. Chem. Soc.* **2018**, *140*, 9551–9557.

[14] M. Liu, W. Wenzel, H. Frisch, *Polym. Chem.* **2020**, *11*, 6616–6623.

[15] P. Zhao, S. Huo, J. Fan, J. Chen, F. Kiessling, A. J. Boersma, R. Göstl, A. Herrmann, *Angew. Chem. Int. Ed.* **2021**, *60*, 14707–14714.

[16] a) J. L. Pelloth, P. A. Tran, A. Walther, A. S. Goldmann, H. Frisch, V. X. Truong, C. Barner-Kowollik, *Adv. Mater.* **2021**, *33*, 2102184; b) A. Chaudhuri, Y. Venkatesh, K. K. Behara, N. P. Singh, *Org. Lett.* **2017**, *19*, 1598–1601; c) N. S. Kosower, E. M. Kosower, G. L. Newton, H. M. Ranney, *Proc. Natl. Acad. Sci. USA* **1979**, *76*, 3382–3386; d) E. M. Kosower, B. Pazhenchevsky, E. Hershkowitz, *J. Am. Chem. Soc.* **1978**, *100*, 6516–6518.

[17] a) N. M. Hamelmann, J. M. Paulusse, *J. Controlled Release* **2023**, *356*, 26–42; b) A. J. Horsfall, D. P. McDougal, D. B. Scanlon, J. B. Bruning, A. D. Abell, *ChemBioChem* **2021**, *22*, 2711–2720; c) A. M. Jones Brunette, D. L. Farrens, *Biochemistry* **2014**, *53*, 6290–6301.

[18] M. Dietrich, M. Glassner, T. Gruendling, C. Schmid, J. Falkenhagen, C. Barner-Kowollik, *Polym. Chem.* **2010**, *1*, 634–644.

Manuscript received: June 30, 2023
Accepted manuscript online: July 23, 2023
Version of record online: ■■, ■■

Research Articles

Polymer Folding

P. H. Maag, F. Feist, V. X. Truong, H. Frisch,* P. W. Roesky,* C. Barner-Kowollik* **e202309259**

Visible-Light-Induced Control over Reversible Single-Chain Nanoparticle Folding

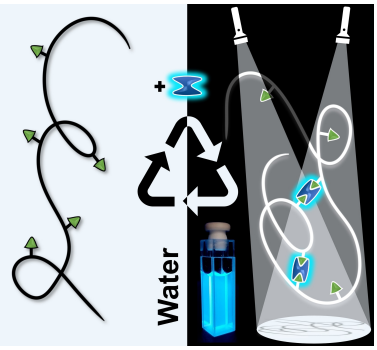

Bimanes allow the synthesis of water-soluble single-chain nanoparticles (SCNPs) and enable the effective unfolding with mild visible light from a compact structure into a linear chain. The unfolding of the fluorescent nanoparticles is reversible and occurs in aqueous systems, making it promising for controlling and tracing the SCNPs in biological environments.